

# DSIC: Dynamic Sample-Individualized Connector for Multi-Scale Object Detection

Zekun Li<sup>2,3</sup>, Yufan Liu<sup>1,2,3</sup>, Bing Li<sup>1,2,3</sup>, Weiming Hu<sup>1,2,3</sup>

<sup>1</sup>CAS Center for Excellence in Brain Science and Intelligence Technology. <sup>2</sup>National Laboratory of Pattern Recognition, Institute of Automation, Chinese Academy of Sciences  
<sup>3</sup>School of Artificial Intelligence, University of Chinese Academy of Sciences, Beijing 100190

## Abstract

Although object detection has reached a milestone thanks to the great success of deep learning, the scale variation is still the key challenge. Integrating multi-level features is presented to alleviate the problems, like the classic Feature Pyramid Network (FPN) and its improvements. However, the specifically designed feature integration modules of these methods may not have the optimal architecture for feature fusion. Moreover, these models have fixed architectures and data flow paths, when fed with various samples. They cannot adjust and be compatible with each kind of data. To overcome the above limitations, we propose a Dynamic Sample-Individualized Connector (DSIC) for multi-scale object detection. It dynamically adjusts network connections to fit different samples. In particular, DSIC consists of two components: Intra-scale Selection Gate (ISG) and Cross-scale Selection Gate (CSG). ISG adaptively extracts multi-level features from backbone as the input of feature integration. CSG automatically activate informative data flow paths based on the multi-level features. Furthermore, these two components are both plug-and-play and can be embedded in any backbone. Experimental results demonstrate that the proposed method outperforms the state-of-the-arts.

## Introduction

Object detection has been explored for many years as a foundation in computer vision. With the great development of deep learning, object detection has achieved remarkable progress. Plenty of excellent detectors (Girshick et al. 2014; Girshick 2015; Ren et al. 2015; Redmon et al. 2016; Liu et al. 2016) are proposed to improve the performance and show extraordinary results on public benchmarks such as *MS – COCO* (Lin et al. 2014).

However, there are still some problems limiting the performance of detectors. Scale variation is one of the most challenging problems. Feature pyramid Network (FPN) (Lin et al. 2017a) is an effective method to alleviate this problem by merging features at adjacent levels to construct a top-down pyramid (seen as Fig 1 (a)). More recently, some studies (Liu et al. 2018; Sun et al. 2019; Pang et al. 2019) have been proposed to improve the connection design in FPN. Nevertheless, the manual designed architectures have

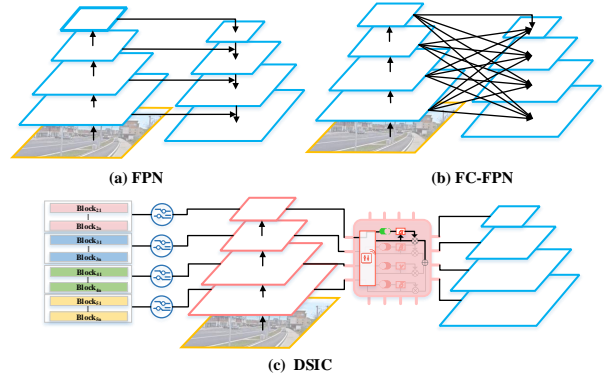


Figure 1: Illustrations of the classical Feature Pyramid Network (FPN) (a), Fully-Connected FPN (FC-FPN) (b) and our method Dynamic Sample-Individualized Connector (DSIC) (c). FPN and FC-FPN represent the different cases of connection which use the same output of backbone as input, constantly. Our DSIC can learn to select input from backbone and activate different data flow paths as connection according to the input sample.

fixed connections, ignoring the diversity brought by different samples. And the interaction across multi-level features is not adequate, because the specific connections cannot be the optimal case in various situations.

Fully-Connected Feature Pyramid Network (FC-FPN), depicted in Fig 1 (b), can be seen as the universal set that includes all connection methods between the bottom-up and top-down pyramid. It use full connection to enhance the feature representation without manual design. But meanwhile, redundancy and noise are brought in, which is unnecessary to utilize all levels everytime. Furthermore, both FPN with its improvements and FC-FPN are fixed, which is not friendly to each sample.

In this paper, in order to address aforementioned problems, we propose a novel and effective module called Dynamic Sample-Individualized Connector (DSIC). Different from the methods mentioned above (i.e., Fig 1(a) and (b)), DSIC dynamically select the proper input and connections, like Fig 1(c) illustrated. It avoids fixed specific design, and automatically adjust the connection and feature interaction process, to fit different samples. In particular, we firstly

present a gate operator as the basic element of DSIC, which controls the state of data flow path. Given control signals, it can connect or disconnect a data flow path, even further enhance or suppress the data flow. Based on the gate operator, DSIC is constructed, which consists of two components: Intra-scale Selection Gate (ISG) and Cross-scale Selection Gate (CSG). ISG aims to explore what is the proper input of feature integration. It can adaptively extract multi-level features with sufficient information from backbone. CSG devotes to learning how to connect multi-level features to obtain an optimal feature integration result. It automatically activate informative data flow paths based on the multi-level features. Furthermore, these two components are both plug-and-play and can be embedded in any backbones.

In summary, this work makes the following main contributions:

- We propose a novel plug-and-play block called DSIC to address the scale-variant problem which makes the utilization of multi-level features more generalized. To control the connection of data flow path dynamically, we firstly present the gate operator as the basic element of DSIC. It is the core operation of the proposed method.
- We propose Intra-scale Selection Gate (ISG) and Cross-scale Selection Gate (CSG) to constitute DSIC, taking advantage of the presented gate operator. ISG aims to adaptively extracts multi-level features from backbone as input, while CSG devotes to automatically activate informative data flow paths based on the multi-level features. Each of these components can be separately embedded into any backbones.
- We evaluate the proposed framework on *MS – COCO2017* and it shows the superiority when compared with state-of-the-arts. The extension ablation experiments validate the effectiveness of two modules in our DSIC framework.

## Related Works

**Object detection** Recently, object detection has reached a milestone, thanks to the great success of Deep Learning (DL). In terms of detection process, most DL-based detectors can be divided into two types: two-stage detectors (Girshick et al. 2014; Girshick 2015; Ren et al. 2015; Dai et al. 2016; Cai and Vasconcelos 2018) and one-stage detectors (Redmon et al. 2016; Liu et al. 2016; Lin et al. 2017b; Redmon and Farhadi 2018; Zhang et al. 2018). Two-stage detectors show superiority in accuracy and one-stage detectors have a great advantage in speed. All of the above methods use multi-scale anchor boxes to locate the object. More recently, anchor-free detectors (Law and Deng 2018; Yang et al. 2019; Tian et al. 2019; Duan et al. 2019) that removed the pre-defined anchor boxes have been proposed. These methods leverage the key points, instead of anchor boxes, to predict object localization and classification. After that, ATSS (Zhang et al. 2020c) was proposed to break down barrier between anchor-based and anchor-free detectors through appropriate sample selection.

**Multi-level feature extraction** Scale variation of object instances is a gargantuan obstacle in object detection. The integration of multi-level features is beneficial to mitigate such problem. FPN (Lin et al. 2017a), which uses a feature pyramid to merge two adjacent layers from top to bottom, was designed to extract and fuse multi-scale features. It had achieved significant progress and had been widely used. After that, a series of works were presented with improved structures based on FPN, to further enhance the performance. For example, in terms of structure design, PANet (Liu et al. 2018) improved FPN by adding a new bottom-up structure after the feature pyramid to shorten information path. FPG (Chen et al. 2020b) was proposed utilizing a deep multi-pathway feature pyramid that repeated the fusion process in different directions. HRNet (Sun et al. 2019) maintained the high-resolution features during the forward propagation and designed the parallel connection between different levels. Apart from network structure improvement, some other works devoted to the multi-level feature refinement. For instance, Libra R-CNN (Pang et al. 2019) integrated and refined the features by Gaussian non-local attention to solve the imbalance between high-level and low-level features. Although the methods above have obtain some progress, there are still some problems. The multi-level features extracted from backbone and data flow paths of integration in these networks are fixed, when different inputs and features are being processed. This is not flexible.

**Dynamic Mechanisms** More recently, dynamic mechanisms have been explored to improve the performance of models in computer vision tasks, which adaptively adjust some variables or settings of the network. Some methods use dynamic mechanism to adjust the network configurations. DRConv (Chen et al. 2020a) assigned filters to learning appointed spatial areas that achieved better performance through obtaining rich and diverse spatial information. Other methods dynamically learn to set the hyperparameters. Dynamic R-CNN (Zhang et al. 2020b) was proposed to alleviate the inconsistency between the hyperparameters and training procedure, by automatically adjusting the IoU threshold and the parameters of loss function. Besides, DRHs (Pan et al. 2020) designed a refinement structure for detection head of classification and regression to make the model learn the particularity of different objects. Nevertheless, the existing dynamic mechanisms only focus on training or network configurations adjustment, ignoring the feature settings and data flow path selection. We propose a new dynamic sample-individualized connector that can select the superior features in multi blocks from backbone and the optimal multi-level feature integration strategy when processing different samples dynamically.

## The Proposed Method

In this section, the foundation of the propose method is firstly introduced, including the pipeline and the proposed gate operator. Secondly, Intra-scale Selection Gate (ISG) is constructed to determine the optimal input of feature integration. Subsequently, Cross-scale Selection Gate (CSG) is presented to integrate features more properly. The two com-

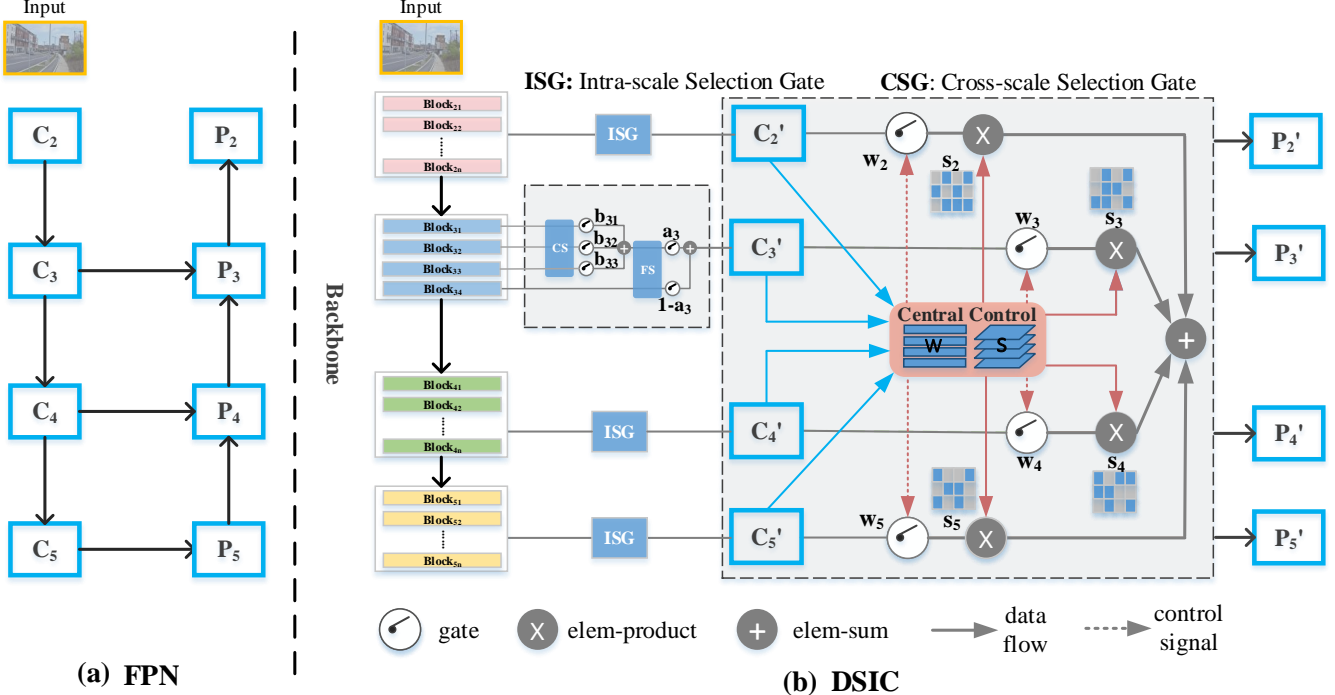


Figure 2: (a) The conventional feature pyramid network. (b) The framework of the proposed DSIC

ponents, i.e., ISG and CSG, constitute the proposed DSIC.

## Foundation

**Pipeline** Existing feature pyramid module is shown in Fig 2 (a), which aims to integrating multi-level features to solve multi-scale object detection. In this module,  $\{C_2, C_3, C_4, C_5\}$  represent the inputs of the feature pyramid. Note that,  $C_i$  is extracted from the output of the  $i$ -th stage of the backbone. In addition,  $\{P_2, P_3, P_4, P_5\}$  represent the new feature maps after feature integration.  $P_k$  denotes the new feature map at the  $k$ -th level. Due to the success of alleviating the scale variation problem, feature pyramid module is widely used in the recent years. However, this module has fixed the input and connection data flow path.

We embed DSIC in the feature integration module to dynamically construct the connection, as illustrated in Fig 2(b). In particular, the proposed DSIC comprises two components: ISG and CSG. ISG is put in the left of the feature integration module, utilized to select the proper features in each stage of the backbone. Note that  $Block_{ij}$  denotes the  $j$ -th block in the  $i$ -th stage. Besides, CSG is leverage to replace the original connection, to obtain an optimal connection cross variant-scale features. We verify in the experiments that there is no need to connect the new generated feature maps (i.e.,  $P_2, P_3, P_4, P_5$ ), thanks to DSIC.

**Gate Operator** The gate operator is the basic element of DSIC, which controls the data flow path. In detail, given data flow  $\mathbf{X} \in \mathbb{R}^{c \times h \times w}$  as input, the gate operator  $\mathcal{G}(\cdot)$  can be formulated as:

$$\mathcal{G}(\varepsilon, \mathbf{X}) = \sigma[\Psi(\varepsilon, \sum_{\Phi \in \mathcal{F}} \Phi(\mathbf{X}))], \quad (1)$$

in which  $\varepsilon \in \mathbb{R}^{m \times 1 \times 1}$  denotes the gate control signal. It assists the gate to determine whether to open or close, and further enhance or suppress the data flow when the gate is open.  $\mathcal{F}$  represents the set of functions, including a series of convolutions, making the input compatible with the gate.  $\Psi(\cdot)$  denotes the Hadamard product and  $\sigma(\cdot)$  represents the mode selection of gate operator by activation function. In this manner, given different data and control signals, the gate shows different states so that the input and connection data flow paths are dynamically changed.

## Intra-scale Selection Gate (ISG)

The input with sufficient information is crucial to feature integration. The conventional FPN only extracts the feature maps from each stage's last block as input. This design is rigid, in which only single block's output is used while the information of the rest is lost. Contrastively, we propose ISG to dynamically select the intra-scale information in backbone from coarse to fine and obtain an input with adequate information.

As shown in Fig 2 (b), ISG is comprised by two phases: Coarse Selection (CS) and Fine Selection (FS). Because of the stronger representation of last block, CS at first selects the useful information from  $(n-1)$  former blocks, to compensate the information that the last block lacks. FS further selects a proper fusion of the last block's output and the complementary data.

In particular, the  $(n-1)$  former blocks  $\{B_{ij}\}_{j=1}^{j=n-1}$  in the  $i$ -th stage are fed into CS, and then the corresponding control

signals  $b_{ij}$  are obtained to adjust the states of the gates:

$$\{b_{i1}, \dots, b_{ij}\} = \sum_{\Phi \in \mathcal{I}} \Phi \{B_{i1}, \dots, B_{ij}\}, \quad j = (1, 2, \dots, n-1), \quad (2)$$

where  $\mathcal{I}$  denotes set of integration operators, including channel-wise concatenation, a series of convolutions and poolings. Note that the parameters of CS in each stage are non-shared. After that, given outputs of blocks and control signals, a series of gates control the data flow paths and obtain:

$$B_i^{CS} = \sum_{j=1}^{n-1} \mathcal{G}(b_{ij}, B_{ij}). \quad (3)$$

The gate operators  $\mathcal{G}(\cdot)$  control whether the data flows from some blocks are needed currently.  $B_i^{CS}$  denotes the result of selection from previous output. After the process of CS, the results are fed into FS to select an integration of  $B_{i,n}$  and  $B_i^{CS}$ . Similarly, considering  $B_{i,n}$  and  $B_i^{CS}$ , FS computes the gate control signals  $a_i$ :

$$a_i = \text{Max}[\tanh(F_{gap}(B_{i,n-1}) + F_{gmp}(B_{i,n-1})), 0], \quad (4)$$

where  $\tanh$  denotes the Tanh activation operator and  $F_{gap}$  and  $F_{gmp}$  means global average-pooling and global max-pooling, respectively. Here,  $a_i \in \mathbb{R}^{c \times 1 \times 1}$  is the control signals of  $B_i^{CS}$  that determines which channels should pass in the gate operator. After the computation of FS, the dynamically selected input of feature integration  $C'_i$  can be obtained:

$$C'_i = \mathcal{G}(a_i, B_i^{CS}) + \mathcal{G}((1 - a_i), B_{i,n}). \quad (5)$$

Instead of the fixed input of FPN, we rethink the effect of all blocks in backbone and rearrange the retention and abandon of information. The proposed ISG achieves coarse-to-fine selection, which can dynamically extract the useful information as input according to various samples in backbone. Besides, the fine selection achieves channel-aware selection of different objects. As mentioned before, our ISG solve the problem of what is the proper input of fusion process and can be put in every feature integration module.

### Cross-scale Selection Gate (CSG)

In multi-scale object detectors, feature integration module merges multi-level feature maps  $\{C'_2, C'_3, C'_4, C'_5\}$  via lateral connections, in order to obtain a feature pyramid  $\{P'_2, P'_3, P'_4, P'_5\}$  with rich semantics at all levels. As shown in Fig 1(b), the full connection in FC-FPN can be seen as the universal set of the lateral connections. This case seems to fully integrate features, but there exist large redundancy. As a result, this case brings in lots of noises and extra computations, which may harm the final performance. On the other hand, the conventional FPN (seen in Fig2 (a)) is the subset of FC-FPN. It only connects the features at the same level from bottom-up pyramid to top-down pyramid in lateral direction. In the vertical direction, FPN only connects features at adjacent levels in a top-down pathway. This architecture is

fixed and is not the optimal case, when it is fed with different samples.

Different from the cases above, we propose CSG to dynamically activate useful data flow paths, and obtain an optimal connection case when meeting various samples. In detail, as illustrated as Fig 2(b), taking  $\{C'_2, C'_3, C'_4, C'_5\}$  as input, the central control unit  $\mathcal{CCU}(\cdot)$  firstly generates gate control signals  $\mathbf{w}_k = \{w_{ik}\}_{i=2}^5$  and pixel-wise selection maps  $\mathbf{s}_k = \{s_{ik}\}_{i=2}^5$ :

$$\{\mathbf{w}_k, \mathbf{s}_k\} = \mathcal{CCU}(\{\mathbf{M}_k\}) \quad k = (2, 3, 4, 5), \quad (6)$$

$$M_{ik} = \begin{cases} F_{down}^{(k-i)}(C'_i) & i < k \\ C'_i & i = k \\ F_{up}^{(i-k)}(C'_i) & i > k \end{cases} \quad (7)$$

Note that  $\mathbf{M}_k = \{M_{ik}\}_{i=2}^5$  is the input feature map with unified resolution. Specifically, to compute  $M_{ik}$ , higher-resolution features are down-sampled by the  $3 \times 3$  convolution and lower-resolution features are up-sampled by bilinear interpolation with appropriate scale factors. In Equation 7,  $F_{down}^{k-i}$  is  $3 \times 3$  convolution operators with  $(k-i)$  times and  $F_{up}^{i-k}$  is bilinear interpolation with scale factor of  $(i-k)$ .

More detailedly, inside the central control unit, the gate control signals  $\{w_{ik}\}_{i=2}^5$  are computed as:

$$\{w_{ik}\}_{i=2}^5 = \sum_{\Phi \in \mathcal{O}_1} \Phi(\{M_{ik}\}_{i=2}^5). \quad (8)$$

$\mathcal{O}_1$  indicates the operation set, including several convolutions and activate functions. The gate control signals  $w_k$  are utilized to adjust the corresponding gate units, so that the useful data flow path can be connected. After the data flow passes the gate, a pixel-wise selection map generated by the central control unit is leveraged to activate the data flow spatially, and further make features from different levels consistent. When it comes to different data flows, the generated selection maps have different activated pixels and significant regions. In particular, inside the central control unit, the pixel-wise selection maps  $\mathbf{s}_k = \{s_{ik}\}_{i=2}^5$  at the  $k$ -th level:

$$\{s_{ik}\}_{i=2}^5 = \sum_{\Phi \in \mathcal{O}_2} \Phi(\{M_{ik}\}_{i=2}^5) \quad (9)$$

$\mathcal{O}_2$  contains a modulus operator that normalize  $M_{ik}$  spatially and a series of operations, including convolutions, activation functions and element-wise sum. Subsequently, the final feature pyramid output can be calculated as:

$$P'_k = \left[ \sum_{i=2}^5 (\mathcal{G}(w_{ik}, M_{ik}) \cdot s_{ik}) \right], \quad (10)$$

where  $P'_k$  denotes the output at the  $k$ -th level, containing rich information at all levels.

To sum up, CSG takes features at all levels into consideration, and automatically select different connections when meeting different samples. This connection case can eliminate redundant information and achieve a better performance, compared with the full connection case. Besides, the

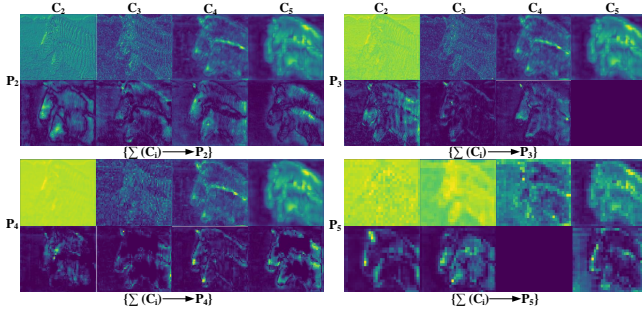


Figure 3: The visual features of our method and FC-FPN.  $C_i$  means the input level and  $P_i$  means the output level. The first row in each level represents the features from FC-FPN, while the features in second row are extracted from our DSIC.

danqishi zhege shi zai maskxia zuode ,bushi faster r50zuode

pixel-wise selection can further refine the passed data flow spatially. Moreover, CSG contains the dynamic vertical connection implicitly which there is no need to connect the new generated feature maps. Hence, features with powerful representation and multi-level information can be obtained to detect the objects accurately.

## Experiments

In this section, we will demonstrate the effectiveness of our DSIC with substantial experiments. We will introduce the dataset and implementation details. Then we will conduct the complete experiments to show superiority and ablation studies to prove the effect of each component. Finally, we will give the detailed and abundant analyses of the experiments.

## Settings

**Data and Evaluation** Our experiments are implemented on MS-COCO 2017 which is a challenging and credible dataset containing 80 object categories. It consists of 115k images for training (*train2017*), 5k images for validation (*val2017*) and 20k test-dev images(*testdev*). The training process is performed on *train2017*, and conduct ablation experiments and final results on *val2017* and *testdev* respectively. The performance is evaluated by standard COCO-style Average Precision (AP) metrics with different IoU thresholds.

**Implementation Details** In order to ensure the fairness of the experiment comparisons, we implement our method and re-implement baseline methods based on PyTorch(Paszke et al. 2017) and mmdetection(Chen et al. 2019). The input images are resized which the shorter size is 800 pixels and the long size is less than 1333 in our configuration. The initial learning rate is 0.02 and it decreases by 0.1 after 8 and 11 epochs respectively. Momentum and weight decay are separately set as 0.9 and 0.0001. The backbones used in our experiments are pre-trained in ImageNet.

Table 1: Comparison of DSIC with baselines(FCOS, Faster R-CNN and Mask R-CNN) on COCO *val2017*. "DSIC" denotes our method. "√" means the baseline models integrated with our connector and others means the baseline models integrated with FPN by default.

Method	Backbone	DSIC	AP	AP <sub>50</sub>	AP <sub>75</sub>	AP <sub>S</sub>	AP <sub>M</sub>	AP <sub>L</sub>
FCOS	ResNet-50	√	36.6	55.7	38.8	20.7	40.1	47.4
	ResNet-101	√	<b>37.7</b>	<b>56.5</b>	<b>40.0</b>	<b>22.1</b>	<b>41.2</b>	<b>48.8</b>
Faster R-CNN	ResNet-50	√	39.2	<b>58.8</b>	42.1	22.9	42.8	<b>51.6</b>
	ResNet-101	√	<b>40.0</b>	58.4	<b>43.1</b>	<b>23.9</b>	<b>43.9</b>	51.2
Mask R-CNN	ResNet-50	√	36.3	58.4	39.1	21.5	40.0	46.6
	ResNet-101	√	<b>38.3</b>	<b>59.7</b>	<b>41.7</b>	<b>22.5</b>	<b>41.7</b>	<b>49.5</b>

## Performance

**Comparison with the baseline** In order to demonstrate the generality of our method, we apply our framework to three common object detectors as our baseline models, including FCOS(Tian et al. 2019), Faster R-CNN (Ren et al. 2015) and Mask R-CNN(He et al. 2017). We utilize ResNet-50 and ResNet-101 with FPN as backbone for the sake of proving the effectiveness of our method. We integrate our method to three models which makes the feature integration and interaction more generalized. Besides, for a fair comparison, we re-implement the corresponding baselines equipped with FPN on mmdetection and report the results of them which have better performance than that were reported in papers generally.

As shown in Table 1, the comparison results are evaluated on *val2017* without the bells and whistles. Our DSIC achieves consistent improvement overall all baseline detectors. Our method achieves 38.3 and 39.6 AP for Faster R-CNN with FPN when using ResNet-50 and ResNet-101 as backbone, respectively. We also evaluate our method on Mask R-CNN, which is improved by 1.5 AP on the detection task with ResNet-50. While for the one stage model FCOS, our method improves 1.1 and 0.8 AP on ResNet-50 and ResNet-100 when compared to the baseline. Thus, our method brings the definite improvements on various public backbone and different detectors. The better performance proves the generalization and robustness ability of DSIC.

**Comparison with other feature fusion modules** As shown in Table 2, we compare our method with other different feature fusion modules on Faster R-CNN with ResNet-50. It is obvious that DSIC provides the optimal performance increase when compared to common feature pyramid networks including PANet (Liu et al. 2018), FPT (Zhang et al. 2020a) and FPG (Chen et al. 2020b). We dynamically select different connections according to inputs avoiding the contradiction between redundant information in fully-connected FPN. When it comes to ASFF (Liu, Huang, and Wang 2019), our method abandon the FPN in framework and consider the global information with better feature selection. So our method can make feature fusion more general and flexible. Results of comparison demonstrate the effectiveness of our method in feature fusion. Besides, we extract the features in every level from FC-FPN and our DSIC to comparison. As shown in Fig 3, the information in different input levels

Table 2: Comparison with other feature fusion methods on Faster R-CNN with ResNet-50. The performance is evaluated on COCO *val2017*.

Fusion method	<i>AP</i>	<i>AP<sub>50</sub></i>	<i>AP<sub>75</sub></i>	<i>AP<sub>S</sub></i>	<i>AP<sub>M</sub></i>	<i>AP<sub>L</sub></i>
FPN	36.3	58.4	39.1	21.5	40.0	46.6
FC-FPN	37.5	59.1	40.3	21.8	41.4	48.7
ASFF	37.5	59.1	40.5	21.6	41.4	48.6
PANet	37.7	59.5	40.7	21.8	41.5	48.9
FPG	38.0	59.4	41.2	22.1	40.7	46.4
FPT	38.0	57.1	38.9	20.5	38.1	<b>55.7</b>
Ours	<b>38.3</b>	<b>59.7</b>	<b>41.7</b>	<b>22.5</b>	<b>41.7</b>	49.5

is complementary instead of redundant repetition which can focus on region of interest.

**Comparison with State-of-the-art** In this section, we evaluate our detector on COCO *test-dev* set and compare with other state-of-the-art object detection approaches. For a fair comparison, we re-implement the corresponding baselines equipped with FPN on mmdetection and the performance of all methods is based on single-model inference. Besides, we use 2x training scheme without any bells and whistles to train our method on Faster R-CNN and Mask R-CNN. All results are shown in Table 3.

It is obvious that our DISC boosts the baselines by a significant improvement when integrated with one-stage and two-stage detectors. Also, our method outperforms the state-of-the-art detectors based on the same backbone without any bells and whistles. These improvements demonstrate the superior performance of our proposed framework.

## Ablation Studies

In this section, we analyze the effects of each components in our proposed method with extensive ablation experiments. And the corresponding results are analyzed as well. We conduct the ablation experiments on *val2017*, using Faster R-CNN with FPN based on ResNet-50.

**Ablation studies on each component** In order to verify the importance of our components in DSIC, we apply the ISG and CSG to the model gradually. The baseline method for our all ablation studies is Faster R-CNN with FPN based on ResNet50. We report the overall ablation studies in Table 4. "CSG" means our method abandons the FPN when compared to the baseline.

**Ablation studies on Intra-scale Selection Gate** In this section we discuss the different hyper-parameter settings in backbone. There are many blocks in ResNet-50 and ResNet-101. Thus we set the different sampling strides of backbone considering the computation cost. When stride is "1", all blocks are applied to selection. "2" means that we take samples from the last block to the formers with stride of 2. The experiment results shown in Table 5 present the performance with different sampling strides in ResNet-50 and ResNet-101. Using all blocks shows better result than taking samples with stride of 2 in both two backbones, almost without additional cost. Hence sufficient information can make detectors have a full choice and our ISG can be embedded into other feature fusion method with cost-free improvement. All

blocks are applied to selection in both two backbones by default.

In addition, we discuss the necessity of fine selection in our method. FS aims to evaluate the importance of information from the last block and coarse selection in channel level. As shown in Table 6, we conduct the experiment of dealing with all blocks in the same way without fine selection based on Faster R-CNN with FPN. The baseline is Faster R-CNN with FPN on ResNet-50. The method with FS achieves better performance which validates the effectiveness of channel-aware selection.

**Ablation studies on Cross-scale Selection Gate** FPN as a classic and basic solution for multi-level features extraction is widely used as a important part in many studies. Thus, we analyze the necessity of FPN in our method. As presented in Table 7, the baseline is the Faster R-CNN with FPN. "Inside FPN" denotes that we replace the lateral connections in FPN with CSG. "After FPN" represents adding our method after the top to down pyramid of FPN. Both of their performance validate the superiority of our cross-scale selection gate. However, our method applied to baseline alone achieves best performance. Because CSG selects the proper path for input samples which eliminates the redundant information and contains the dynamic vertical connection implicitly. Thus, cross-scale selection gate can also become a plugged module applied to any models replacing FPN.

**Ablation studies on Gate operator** We further consider the mode selection in gate operator of two selection gate modules. Experiments results with different modes in two modules are shown in Table 8. In ISG, the three modes achieve the similar result which Softmax and Sigmoid ignore the noise in redundant information, which Tanh has a better performance. We consider the information in the same stage is more complementary instead of mutual exclusion. However, in CSG, the performance of three modes has obvious differences because of spatial contradiction of different levels. We consider that the Softmax operator takes account of four levels' data flow together ignoring the independence and the inconsistency. Sigmoid considers the data flow individually but it can't eliminate the redundant information. Tanh avoids the above defects and achieves the best result. Thus we select the Tanh as our mode in two selection gate modules by default.

**Visualization** Moreover, we present the visual results of our method in CSG. AS shown in Fig 4, three different samples tend to select different connections according to the scale of objects, which validates the sample-individualized data flow path selection of our method. In addition, we find that the regression task need more high-resolution information whether large or small scale samples. But the highest-resolution information is from the other three levels instead of itself which contains huge noise. By contrast, the classification task need more semantic information from itself. Our method dynamically selects the input and data flow paths of feature integration which reconciles the differences between the classification and regression to some extent.

Table 3: Comparisons with the state-of-the-art methods on COCO *test – dev*. The symbol “\*” means our re-implemented results on mmdetection.

Method	Backbone	Schedule	AP	AP <sub>50</sub>	AP <sub>75</sub>	AP <sub>S</sub>	AP <sub>M</sub>	AP <sub>L</sub>
YoLOv2(Redmon and Farhadi 2017)	DarkNet-19	-	21.6	44.0	19.2	5.0	22.4	35.5
SSD512(Liu et al. 2016)	ResNet-101	-	31.2	50.4	33.3	10.2	34.5	49.8
CornerNet(Law and Deng 2018)	Hourglass-104	-	40.6	56.4	43.2	19.1	42.8	<b>54.3</b>
Faster R-CNN(Ren et al. 2015)	ResNet-101-FPN	-	36.2	59.1	39.0	18.2	39.0	48.2
Deformable R-FCN(Dai et al. 2016)	Inception-ResNet-v2	-	37.5	58.0	40.8	19.4	40.1	52.5
Mask R-CNN(He et al. 2017)	ResNet-101-FPN	-	38.2	60.3	41.7	20.1	41.1	50.2
Libra R-CNN(Pang et al. 2019)	ResNet-101-FPN	1x	40.3	61.3	43.9	22.9	43.1	51.0
RetinaNet*	ResNet-50-FPN	1x	35.8	55.6	38.4	19.8	38.8	45.0
FCOS*	ResNet-101-FPN	2x	40.9	60.2	44.1	24.7	45.0	52.3
Faster R-CNN*	ResNet-101-FPN	2x	39.5	59.9	43.0	22.4	43.1	52.5
Mask R-CNN*	ResNet-101-FPN	2x	40.8	62.1	44.6	22.8	43.9	52.0
DSIC RetinaNet(ours)	ResNet-50-FPN	1x	37.2	57.3	39.8	20.3	40.0	47.1
DSIC FCOS(ours)	ResNet-101	2x	41.6	60.8	44.8	25.4	45.5	53.5
DSIC Faster R-CNN(ours)	ResNet-101	2x	41.0	60.4	44.5	25.0	44.7	52.6
DSIC Mask R-CNN(ours)	ResNet-101	2x	<b>42.6</b>	<b>63.0</b>	<b>46.6</b>	<b>25.5</b>	<b>46.4</b>	54.0

Table 4: Effect of each component. Results are evaluated on COCO *val2017*. ISG: Intra-scale Selection Gate, CSG: Cross-scale Selection Gate.

Method	AP	AP <sub>50</sub>	AP <sub>75</sub>	AP <sub>S</sub>	AP <sub>M</sub>	AP <sub>L</sub>
baseline	36.3	58.4	39.1	21.5	40.0	46.6
baseline+ISG	37.6	59.0	40.5	21.7	40.9	49.0
baseline+CSG	37.8	59.1	41.0	21.8	<b>41.8</b>	48.9
baseline+ISG+CSG	<b>38.3</b>	<b>59.7</b>	<b>41.7</b>	<b>22.5</b>	41.7	<b>49.5</b>

Table 5: Comparison with different sample strides in backbone. The performance is evaluated on COCO *val2017* and FLOPS are reported on a single image of size 1280×800.

Backbone	Stride	AP	AP <sub>50</sub>	AP <sub>75</sub>	FLOPS(G)
ResNet-50	baseline	36.3	58.4	39.1	<b>207.07</b>
	1	<b>37.6</b>	59.0	40.5	207.21
	2	37.3	58.9	40.5	207.17
ResNet-101	baseline	38.3	60.1	41.7	<b>283.14</b>
	1	<b>39.3</b>	60.8	42.4	283.36
	2	39.0	60.6	42.3	283.31

Table 6: Comparison with whether to apply the fine selection on Faster R-CNN with FPN. “FS” means the fine selection. The performance is evaluated on COCO *val2017*.

Fusion method	AP	AP <sub>50</sub>	AP <sub>75</sub>	AP <sub>S</sub>	AP <sub>M</sub>	AP <sub>L</sub>
baseline	36.3	58.4	39.1	21.5	40.0	46.6
ISG w/o FS	37.3	58.8	40.2	21.6	<b>41.0</b>	47.8
ISG w FS	<b>37.6</b>	<b>59.0</b>	<b>40.5</b>	<b>21.7</b>	40.9	<b>49.0</b>

Table 7: Comparison with whether to integrate the FPN on cross-scale selection gate. The performance is evaluated on COCO *val2017*.

Integration method	AP	AP <sub>50</sub>	AP <sub>75</sub>	AP <sub>S</sub>	AP <sub>M</sub>	AP <sub>L</sub>
baseline	36.3	58.4	39.1	21.5	40.0	46.6
After FPN	37.3	58.7	40.6	21.3	41.0	48.8
Inside FPN	37.4	58.9	40.3	21.5	41.5	47.5
CSG(ours)	<b>37.8</b>	<b>59.1</b>	<b>41.0</b>	<b>21.8</b>	<b>41.8</b>	<b>48.9</b>

Table 8: Comparison with different mode selection of two gate modules. The performance is evaluated on COCO *val2017*.

Module	Mode selection	AP	AP <sub>50</sub>	AP <sub>75</sub>	AP <sub>S</sub>	AP <sub>M</sub>	AP <sub>L</sub>
ISG	Softmax	37.4	58.9	<b>40.7</b>	21.6	41.2	48.2
	Sigmoid	37.5	58.7	40.4	21.7	<b>41.3</b>	47.9
	Tanh	<b>37.6</b>	<b>59.0</b>	40.5	<b>21.7</b>	40.9	<b>49.0</b>
CSG	Softmax	37.4	59.0	40.4	21.3	41.0	48.4
	Sigmoid	37.6	<b>59.4</b>	40.4	<b>21.9</b>	41.4	48.8
	Tanh	<b>37.8</b>	59.1	<b>41.0</b>	21.8	<b>41.8</b>	<b>48.9</b>

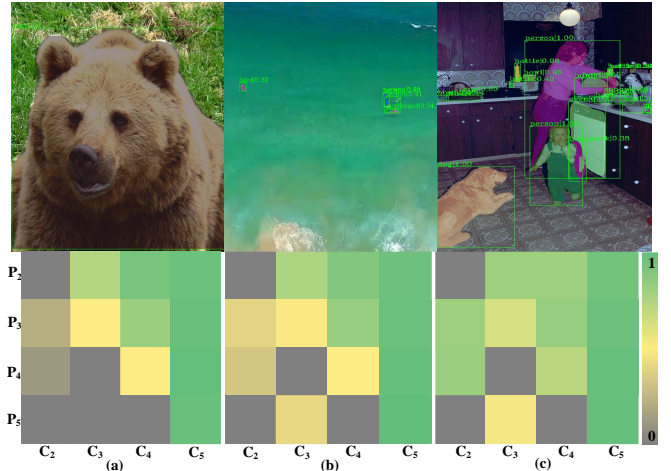


Figure 4: The visual results of our method. The first row is the detection results and the second row is the corresponding state matrix of each data flow path. (a) is the large scale input. (b) is the small scale input. And (c) has various scales of input.

## Conclusion

In this paper, we have proposed a novel dynamic sample-individualized connector for multi-scale object detection, named DSIC, to adjust network connections to fit different samples, dynamically. With the help of two simple yet effective components, Intra-scale selection gate and Cross-scale selection gate, DSIC has shown the generality for both two-stage and single-stage detectors and have a significant improvement. Compared with previous approaches, DSIC offer several advantages: (1) it avoids the special manual design and insufficient interaction among multi levels, whose the whole process is sample-individualized learning; (2) it makes the multi-level feature integration in different computer vision tasks more generalized with the simple implementation. The experiments on *MS – COCO* show the superiority of DSIC.

## References

Cai, Z.; and Vasconcelos, N. 2018. Cascade r-cnn: Delving into high quality object detection. In *Proceedings of the IEEE conference on computer vision and pattern recognition*, 6154–6162.

Chen, J.; Wang, X.; Guo, Z.; Zhang, X.; and Sun, J. 2020a. Dynamic Region-Aware Convolution. *arXiv preprint arXiv:2003.12243*.

Chen, K.; Cao, Y.; Loy, C. C.; Lin, D.; and Feichtenhofer, C. 2020b. Feature Pyramid Grids. *arXiv preprint arXiv:2004.03580*.

Chen, K.; Wang, J.; Pang, J.; Cao, Y.; Xiong, Y.; Li, X.; Sun, S.; Feng, W.; Liu, Z.; Xu, J.; et al. 2019. MMDetection: Open MMLab Detection Toolbox and Benchmark. *arXiv preprint arXiv:1906.07155*.

Dai, J.; Li, Y.; He, K.; and Sun, J. 2016. R-fcn: Object detection via region-based fully convolutional networks. In *Advances in neural information processing systems*, 379–387.

Duan, K.; Bai, S.; Xie, L.; Qi, H.; Huang, Q.; and Tian, Q. 2019. CenterNet: Keypoint Triplets for Object Detection. In *2019 IEEE/CVF International Conference on Computer Vision (ICCV)*, 6568–6577.

Girshick, R. 2015. Fast r-cnn. In *Proceedings of the IEEE international conference on computer vision*, 1440–1448.

Girshick, R.; Donahue, J.; Darrell, T.; and Malik, J. 2014. Rich feature hierarchies for accurate object detection and semantic segmentation. In *Proceedings of the IEEE conference on computer vision and pattern recognition*, 580–587.

He, K.; Gkioxari, G.; Dollár, P.; and Girshick, R. 2017. Mask r-cnn. In *Proceedings of the IEEE international conference on computer vision*, 2961–2969.

Law, H.; and Deng, J. 2018. Cornernet: Detecting objects as paired keypoints. In *Proceedings of the European Conference on Computer Vision (ECCV)*, 734–750.

Lin, T.-Y.; Dollár, P.; Girshick, R.; He, K.; Hariharan, B.; and Belongie, S. 2017a. Feature pyramid networks for object detection. In *Proceedings of the IEEE conference on computer vision and pattern recognition*, 2117–2125.

Lin, T.-Y.; Goyal, P.; Girshick, R.; He, K.; and Dollár, P. 2017b. Focal loss for dense object detection. In *Proceedings of the IEEE international conference on computer vision*, 2980–2988.

Lin, T.-Y.; Maire, M.; Belongie, S. J.; Hays, J.; Perona, P.; Ramanan, D.; Dollár, P.; and Zitnick, C. L. 2014. Microsoft COCO: Common Objects in Context. In *European Conference on Computer Vision*, 740–755.

Liu, S.; Huang, D.; and Wang, Y. 2019. Learning Spatial Fusion for Single-Shot Object Detection. *arXiv preprint arXiv:1911.09516*.

Liu, S.; Qi, L.; Qin, H.; Shi, J.; and Jia, J. 2018. Path aggregation network for instance segmentation. In *Proceedings of the IEEE Conference on Computer Vision and Pattern Recognition*, 8759–8768.

Liu, W.; Anguelov, D.; Erhan, D.; Szegedy, C.; Reed, S.; Fu, C.-Y.; and Berg, A. C. 2016. Ssd: Single shot multibox detector. In *European conference on computer vision*, 21–37. Springer.

Pan, X.; Ren, Y.; Sheng, K.; Dong, W.; Yuan, H.; Guo, X.; Ma, C.; and Xu, C. 2020. Dynamic Refinement Network for Oriented and Densely Packed Object Detection. In *CVPR 2020: Computer Vision and Pattern Recognition*, 11207–11216.

Pang, J.; Chen, K.; Shi, J.; Feng, H.; Ouyang, W.; and Lin, D. 2019. Libra r-cnn: Towards balanced learning for object detection. In *Proceedings of the IEEE Conference on Computer Vision and Pattern Recognition*, 821–830.

Paszke, A.; Gross, S.; Chintala, S.; Chanan, G.; Yang, E.; DeVito, Z.; Lin, Z.; Desmaison, A.; Antiga, L.; and Lerer, A. 2017. Automatic differentiation in pytorch .

Redmon, J.; Divvala, S.; Girshick, R.; and Farhadi, A. 2016. You only look once: Unified, real-time object detection. In *Proceedings of the IEEE conference on computer vision and pattern recognition*, 779–788.

Redmon, J.; and Farhadi, A. 2017. YOLO9000: Better, Faster, Stronger. In *2017 IEEE Conference on Computer Vision and Pattern Recognition (CVPR)*, 6517–6525.

Redmon, J.; and Farhadi, A. 2018. YOLOv3: An Incremental Improvement. *arXiv preprint arXiv:1804.02767* .

Ren, S.; He, K.; Girshick, R.; and Sun, J. 2015. Faster r-cnn: Towards real-time object detection with region proposal networks. In *Advances in neural information processing systems*, 91–99.

Sun, K.; Xiao, B.; Liu, D.; and Wang, J. 2019. Deep high-resolution representation learning for human pose estimation. *arXiv preprint arXiv:1902.09212* .

Tian, Z.; Shen, C.; Chen, H.; and He, T. 2019. FCOS: Fully Convolutional One-Stage Object Detection. In *2019 IEEE/CVF International Conference on Computer Vision (ICCV)*, 9626–9635.

Yang, Z.; Liu, S.; Hu, H.; Wang, L.; and Lin, S. 2019. RepPoints: Point Set Representation for Object Detection. *arXiv preprint arXiv:1904.11490* .

Zhang, D.; Zhang, H.; Tang, J.; Wang, M.; Hua, X.; and Sun, Q. 2020a. Feature Pyramid Transformer. *arXiv: Computer Vision and Pattern Recognition* .

Zhang, H.; Chang, H.; Ma, B.; Wang, N.; and Chen, X. 2020b. Dynamic R-CNN: Towards High Quality Object Detection via Dynamic Training. *arXiv preprint arXiv:2004.06002* .

Zhang, S.; Chi, C.; Yao, Y.; Lei, Z.; and Li, S. Z. 2020c. Bridging the Gap Between Anchor-Based and Anchor-Free Detection via Adaptive Training Sample Selection. In *CVPR 2020: Computer Vision and Pattern Recognition*, 9759–9768.

Zhang, S.; Wen, L.; Bian, X.; Lei, Z.; and Li, S. Z. 2018. Single-shot refinement neural network for object detection. In *Proceedings of the IEEE Conference on Computer Vision and Pattern Recognition*, 4203–4212.